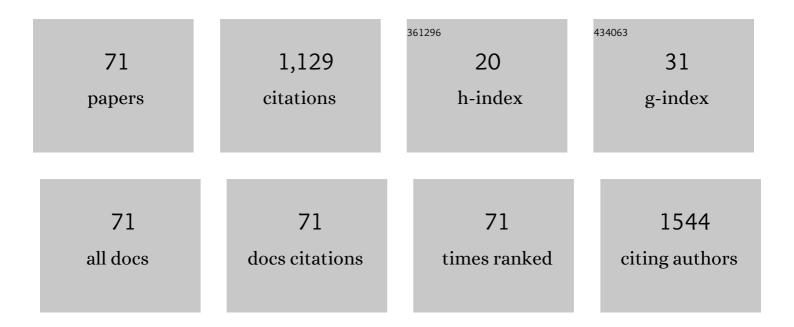
## Xiao Jin

## List of Publications by Year in descending order

Source: https://exaly.com/author-pdf/4822281/publications.pdf Version: 2024-02-01



XIAO LIN

#	Article	IF	CITATIONS
1	Simultaneously Mitigating Anion and Cation Defects Both in Bulk and Interface for Highâ€Effective Perovskite Solar Cells. Solar Rrl, 2022, 6, .	3.1	2
2	Zinc and Acetate Co-doping for Stable Carbon-Based CsPblBr <sub>2</sub> Solar Cells with Efficiency over 10.6%. ACS Applied Energy Materials, 2022, 5, 2720-2726.	2.5	4
3	Controlling the emission linewidths of alloy quantum dots with asymmetric strain. Journal of Colloid and Interface Science, 2022, 624, 287-295.	5.0	2
4	Thick-shell CdZnSe/ZnSe/ZnS quantum dots for bright white light-emitting diodes. Journal of Luminescence, 2021, 229, 117670.	1.5	10
5	White light-emitting diodes based on quaternary Ag–In-Ga-S quantum dots and their influences on melatonin suppression index. Journal of Luminescence, 2021, 233, 117903.	1.5	8
6	High Colorâ€Rendering Index and Stable White Lightâ€Emitting Diodes Based on Highly Luminescent Quantum Dots. Particle and Particle Systems Characterization, 2021, 38, 2100120.	1.2	6
7	High quality quarternary-alloyed ZnCdSSe/ZnS quantum dots with single photoluminescence decay channel and high devise stability. Journal of Luminescence, 2021, 240, 118463.	1.5	4
8	Spectral Design of Light-Emitting Diodes for Plant Photosynthesis Based on Quantum Dots. IEEE Access, 2021, 9, 156229-156238.	2.6	9
9	Efficient Quantum Dot Lightâ€Emitting Diodes Based on Wellâ€Type Thickâ€Shell Cd <i><sub>x</sub></i> Zn <sub>1â^'</sub> <i><sub>x</sub></i> S/CdSe/Cd <i><sub>y</sub></i> Zn <sub>1â^'</sub>	/sub⊅.≇i> <s< td=""><td>subøy</td></s<>	subøy
10	Cation exchange assisted synthesis of ZnCdSe/ZnSe quantum dots with narrow emission line widths and near-unity photoluminescence quantum yields. Chemical Communications, 2020, 56, 6130-6133.	2.2	33
11	One pot synthesis of thick shell blue emitting CdZnS/ZnS quantum dots with narrow emission line width. Optical Materials Express, 2020, 10, 1232.	1.6	7
12	High efficient light-emitting diodes with improved the balance of electron and hole transfer via optimizing quantum dot structure. Optical Materials Express, 2019, 9, 3089.	1.6	6
13	Quaternary quantum dots with gradient valence band for all-inorganic perovskite solar cells. Journal of Colloid and Interface Science, 2019, 549, 33-41.	5.0	19
14	Bright Alloy CdZnSe/ZnSe QDs with Nonquenching Photoluminescence at High Temperature and Their Application to Light-Emitting Diodes. Journal of Nanomaterials, 2019, 2019, 1-8.	1.5	6
15	Blue quantum dot light-emitting diodes with high luminance by improving the charge transfer balance. Chemical Communications, 2019, 55, 3501-3504.	2.2	49
16	The role of deep-red emission CuInS2/ZnS QDs in white light emitting diodes. Semiconductor Science and Technology, 2019, 34, 035025.	1.0	8
17	The Variation of Sediment Bacterial Community in Response to Anthropogenic Disturbances of Poyang Lake, China. Wetlands, 2019, 39, 63-73.	0.7	6
18	White light emitting device based on single-phase CdS quantum dots. Nanotechnology, 2018, 29, 205701.	1.3	17

Χίαο Jin

#	Article	IF	CITATIONS
19	Balancing the Electron and Hole Transfer for Efficient Quantum Dot Light-Emitting Diodes by Employing a Versatile Organic Electron-Blocking Layer. ACS Applied Materials & Interfaces, 2018, 10, 15803-15811.	4.0	67
20	Highâ€Responsivity Photodetectors Based on Formamidinium Lead Halide Perovskite Quantum Dot–Graphene Hybrid. Particle and Particle Systems Characterization, 2018, 35, 1700304.	1.2	46
21	Photovoltaic-targeted photoluminescence lifetime engineering in bright type-II alloy quantum dots. Solar Energy, 2018, 169, 75-83.	2.9	2
22	Bright alloy type-II quantum dots and their application to light-emitting diodes. Journal of Colloid and Interface Science, 2018, 510, 376-383.	5.0	21
23	Integration of green CuInS_2/ZnS quantum dots for high-efficiency light-emitting diodes and high-responsivity photodetectors. Optical Materials Express, 2018, 8, 314.	1.6	22
24	ZnMgO:ZnO composite films for fast electron transport and high charge balance in quantum dot light emitting diodes. Optical Materials Express, 2018, 8, 909.	1.6	30
25	Stretchable silica gel-ZnSe:Mn/ZnS quantum dots for encoding. Optical Materials Express, 2018, 8, 1154.	1.6	5
26	Photodetectors: High-Responsivity Photodetectors Based on Formamidinium Lead Halide Perovskite Quantum Dot-Graphene Hybrid (Part. Part. Syst. Charact. 4/2018). Particle and Particle Systems Characterization, 2018, 35, 1870012.	1.2	0
27	Bright and efficient quantum dot light-emitting diodes with double light-emitting layers. Optics Letters, 2018, 43, 5925.	1.7	6
28	Solid Ligand-Assisted Storage of Air-Stable Formamidinium Lead Halide Quantum Dots via Restraining the Highly Dynamic Surface toward Brightly Luminescent Light-Emitting Diodes. ACS Photonics, 2017, 4, 2504-2512.	3.2	50
29	Emission tunable CdZnS/ZnSe core/shell quantum dots for white light emitting diodes. Journal of Luminescence, 2017, 192, 867-874.	1.5	27
30	Sodium Gadolinium Fluoride Nanophosphor-Based Solar Cells: Toward Subbandgap Light Harvesting and Efficient Charge Transfer. IEEE Journal of Photovoltaics, 2017, 7, 199-205.	1.5	1
31	Enhancing extraction efficiency of quantum dot light-emitting diodes by surface engineering. Optics Express, 2017, 25, 17683.	1.7	20
32	Quantum dot white light emitting diodes with high scotopic/photopic ratios. Optics Express, 2017, 25, 21901.	1.7	26
33	Highly luminescent red emitting CdZnSe/ZnSe quantum dots synthesis and application for quantum dot light emitting diodes. Optical Materials Express, 2017, 7, 3875.	1.6	19
34	Efficient light-emitting diodes based on reverse type-I quantum dots. Optical Materials Express, 2017, 7, 4395.	1.6	11
35	Nd <sub>2</sub> (S, Se, Te) <sub>3</sub> Colloidal Quantum Dots: Synthesis, Energy Level Alignment, Charge Transfer Dynamics, and Their Applications to Solar Cells. Advanced Functional Materials, 2016, 26, 254-266.	7.8	53
36	Ytterbium–erbium ion doped strontium molybdate (SrMoO <sub>4</sub> ): synthesis, characterization, photophysical properties and application in solar cells. Physical Chemistry Chemical Physics, 2016, 18, 33320-33328.	1.3	7

Χίαο Jin

#	Article	IF	CITATIONS
37	Role of ytterbium-erbium co-doped gadolinium molybdate (Gd_2(MoO_4)_3:Yb/Er) nanophosphors in solar cells. Optics Express, 2016, 24, A1276.	1.7	22
38	Efficient charge transfer and utilization of near-infrared solar spectrum by ytterbium and thulium codoped gadolinium molybdate (Gd2(MoO4)3:Yb/Tm) nanophosphor in hybrid solar cells. Physical Chemistry Chemical Physics, 2016, 18, 30837-30844.	1.3	4
39	Tuning the fluorescence lifetime of donor polymers containing different proportion of electron withdrawing groups inhybrid solar cells. Synthetic Metals, 2016, 221, 19-24.	2.1	2
40	Top-down Strategy toward Versatile Graphene Quantum Dots for Organic/Inorganic Hybrid Solar Cells. ACS Sustainable Chemistry and Engineering, 2015, 3, 637-644.	3.2	75
41	Random Terpolymer Designed with Tunable Fluorescence Lifetime for Efficient Organic/Inorganic Hybrid Solar Cells. ACS Applied Materials & Interfaces, 2015, 7, 17408-17415.	4.0	17
42	In situ synthesis of binary cobalt–ruthenium nanofiber alloy counter electrode for electrolyte-free cadmium sulfide quantum dot solar cells. Journal of Power Sources, 2015, 284, 162-169.	4.0	9
43	Reduced energy offset via substitutional doping for efficient organic/inorganic hybrid solar cells. Optics Express, 2015, 23, A444.	1.7	4
44	Energy gradient architectured praseodymium chalcogenide quantum dot solar cells: towards unidirectionally funneling energy transfer. Journal of Materials Chemistry A, 2015, 3, 23876-23887.	5.2	23
45	Tailoring solar energy spectrum for efficient organic/inorganic hybrid solar cells by up-conversion luminescence nanophosphors. Electrochimica Acta, 2015, 182, 416-423.	2.6	11
46	Small bandgap naphthalene diimide copolymers for efficient inorganic–organic hybrid solar cells. RSC Advances, 2015, 5, 2147-2154.	1.7	8
47	Ruthenium cation substitutional doping for efficient charge carrier transfer in organic/inorganic hybrid solar cells. Journal of Power Sources, 2015, 274, 701-708.	4.0	10
48	Reducing the excess energy offset in organic/inorganic hybrid solar cells: Toward faster electron transfer. Applied Catalysis B: Environmental, 2015, 162, 524-531.	10.8	40
49	Efficient electron/hole transport in inorganic/organic hybrid solar cells by lithium ion and molybdenum trioxide codoping. Journal of Power Sources, 2014, 268, 874-881.	4.0	20
50	Efficiency enhancement via tailoring energy level alignment induced by vanadium ion doping in organic/inorganic hybrid solar cells. RSC Advances, 2014, 4, 46008-46015.	1.7	7
51	Core–Shell Nanophosphor Architecture: Toward Efficient Energy Transport in Inorganic/Organic Hybrid Solar Cells. ACS Applied Materials & Interfaces, 2014, 6, 12798-12807.	4.0	21
52	The origin of efficiency enhancement of inorganic/organic Hybrid solar Cells by robust samarium phosphate nanophosphors. Solar Energy Materials and Solar Cells, 2014, 130, 426-434.	3.0	33
53	Exciton Generation/Dissociation/Charge-Transfer Enhancement in Inorganic/Organic Hybrid Solar Cells by Robust Single Nanocrystalline LnP <sub><i>x</i></sub> O <sub><i>y</i></sub> (Ln = Eu, Y) Doping. ACS Applied Materials & Interfaces, 2014, 6, 8771-8781.	4.0	40
54	Enhanced charge transport and photovoltaic performance induced by incorporating rare-earth phosphor into organic–inorganic hybrid solar cells. Physical Chemistry Chemical Physics, 2014, 16, 24499-24508.	1.3	7

Χίαο Jin

#	Article	IF	CITATIONS
55	Energy level control: toward an efficient hot electron transport. Scientific Reports, 2014, 4, 5983.	1.6	32
56	Third-order nonlinear optical properties of a π-conjugated phenoxazinium compound: Mechanism and dynamic response. Materials Chemistry and Physics, 2013, 139, 975-978.	2.0	10
57	Optical nonlinearity measurement of 4-(N-methyl, N-hydroxyethl)amino, 4′-nitroazobenzene using a transmittance technique with a phase object (T-PO) with top-hat beams at 600-nm wavelength. Chinese Physics B, 2012, 21, 104201.	0.7	Ο
58	Measurements of dynamics of nondegenerate optical nonlinearity in ZnS with pulses from optical parameter generation. Optics Communications, 2012, 285, 1940-1944.	1.0	3
59	Investigation on nonlinear dynamics of ZnO using time-resolved pump-probe technique with phase object. Proceedings of SPIE, 2011, , .	0.8	0
60	Investigation of nonlinear dynamics in CdS by time-resolved nondegenerate pump–probe system with phase object. Journal of Modern Optics, 2011, 58, 973-977.	0.6	3
61	Characterization of signs change of nonlinear refraction in ZnSe based on a modified double 4f imaging system with a phase object. Optics Communications, 2010, 283, 1124-1128.	1.0	9
62	Third-order nonlinearity measurements of PbPc(CP) <sub>4</sub> /DMF. Journal of Optics (United) Tj ETQq0 0 0	rgBT/Ove	rloçk 10 Tf 50
63	Investigation of nonlinear refraction on a thick sample using a simple technique with a phase object. Journal of Physics B: Atomic, Molecular and Optical Physics, 2010, 43, 105401.	0.6	2
64	Solvent effect induced solute damage in an organic inner salt. Optics Express, 2010, 18, 27387.	1.7	4

65	Characterization of the transient thermal-lens effect using top-hat beam Z-scan. Journal of Physics B: Atomic, Molecular and Optical Physics, 2009, 42, 225404.	0.6	8
66	Energy transfer induced by femtosecond two-beam coupling in two Kerr liquids. Journal of Modern Optics, 2009, 56, 2363-2367.	0.6	0
67	Investigation of Two-Photon Absorption Induced Excited State Absorption in a Fluorenyl-Based Chromophore. Journal of Physical Chemistry B, 2009, 113, 15730-15733.	1.2	24
68	Method with a phase object for measurement of optical nonlinearities. Optics Letters, 2009, 34, 2513.	1.7	14
69	Time-resolved pump-probe technology with phase object for measurements of optical nonlinearities. Optics Express, 2009, 17, 7110.	1.7	48
70	Nonlinear absorption measurements using a lens imaging technique. , 2009, , .		0
71	Determination of nonlinear refraction in (TCBD) <inf>2</inf> OPV <inf>3</inf> /CH <inf>2</inf> Cl <inf>2</inf> solution by using the phase-object Z-scan technique. , 2009, , .		0